⌘ *Author's Choice*

THE JOURNAL OF BIOLOGICAL CHEMISTRY VOL. 283, NO. 30, pp. 21160–21169, July 25, 2008
Printed in the U.S.A.

Targeted Disruption of NeuroD, a Proneural Basic Helix-Loop-Helix Factor, Impairs Distal Lung Formation and Neuroendocrine Morphology in the Neonatal Lung*[S]

Received for publication, October 19, 2007, and in revised form, February 12, 2008 Published, JBC Papers in Press, March 13, 2008, DOI 10.1074/jbc.M708692200

Enid R. Neptune[‡§1], Megan Podowski[‡], Carla Calvi[‡], Jang-Hyeon Cho[¶], Joe G. N. Garcia[‡], Rubin Tuder[‖], R. Ilona Linnoila[**], Ming-Jer Tsai[¶], and Harry C. Dietz[§‡‡2]

*From the [‡]Division of Pulmonary and Critical Care Medicine, [§]Institute of Genetic Medicine, [‡‡]Howard Hughes Medical Institute, [‖]Department of Pathology, The Johns Hopkins School of Medicine, Baltimore, Maryland 21205, **Center for Cancer Research, NCI, National Institutes of Health, Bethesda, Maryland 20892, and the [¶]Department of Molecular and Cellular Biology, Baylor College of Medicine, Houston, Texas 77030*

Despite the importance of airspace integrity in vertebrate gas exchange, the molecular pathways that instruct distal lung formation are poorly understood. Recently, we found that fibrillin-1 deficiency in mice impairs alveolar formation and recapitulates the pulmonary features of human Marfan syndrome. To further elucidate effectors involved in distal lung formation, we performed expression profiling analysis comparing the fibrillin-1-deficient and wild-type developing lung. NeuroD, a basic helix-loop-helix transcription factor, fulfilled the expression criteria for a candidate mediator of distal lung development. We investigated its role in murine lung development using genetically targeted NeuroD-deficient mice. We found that NeuroD deficiency results in both impaired alveolar septation and altered morphology of the pulmonary neuroendocrine cells. NeuroD-deficient mice had enlarged alveoli associated with reduced epithelial proliferation in the airway and airspace compartments during development. Additionally, the neuroendocrine compartment in these mice manifested an increased number of neuroepithelial bodies but a reduced number of solitary pulmonary neuroendocrine cells in the neonatal lung. Overexpression of NeuroD in a murine lung epithelial cell line conferred a neuroendocrine phenotype characterized by the induction of neuroendocrine markers as well as increased proliferation. These results support an unanticipated role for NeuroD in the regulation of pulmonary neuroendocrine and alveolar morphogenesis and suggest an intimate connection between the neuroendocrine compartment and distal lung development.

Animal models of Mendelian disorders with multisystem manifestations, such as Marfan syndrome (MFS),[3] represent uniquely instructive tools that can be used to elucidate novel mediators of tissue-specific morphogenic programs. MFS, an autosomal dominant disorder of connective tissue caused by mutations in the extracellular matrix protein fibrillin-1, manifests with cardiovascular, musculoskeletal, ocular, and pulmonary abnormalities. We recently found that fibrillin-1-deficient mice display defects in airspace formation that mimic the lung phenotype observed in a subset of patients with MFS (1). Although MFS is a relatively uncommon disorder, we reasoned that the lung septation abnormalities seen in MFS might involve critically important molecular pathways that normally operate in the prealveolarization stage of distal lung morphogenesis. In this view, we investigated the role of NeuroD, a proneural basic helix-loop-helix (bHLH) factor as a leading candidate mediator of distal lung morphogenesis.

NeuroD is a member of a family of proneural bHLH proteins related by structural motifs that underscore concomitant roles in neural, endocrine, and neuroendocrine development (2). NeuroD family members function as differentiation genes, primarily serving to activate terminal differentiation of resident precursor cells (3). Although the lung exhibits many features of an endocrine/neuroendocrine organ, the role of proneural bHLH factors in lung differentiation and development has only recently been examined (4). Mice with a targeted deletion in Mash1, another proneural bHLH factor, do not develop pulmonary neuroendocrine cells (PNECs) and die in the neonatal period secondary to respiratory failure. Unfortunately, because of early perinatal lethality, the distal lung phenotype cannot be fully characterized in this model. Gene targeting experiments have revealed critical roles for NeuroD in hippocampal, cere-

* This work was supported, in whole or in part, by National Institutes of Health Grants AR41135 (to H. D.), HL-69340 and KO8-HL067980 (to E. R. N.), DK 45641 and HD17379 (to M. J. T.), and RO1HL66554 (to R. M. T.), the Intramural Research Program (to R. I. L.), NCI (to R. I. L.), and U01 HL66583 (to J. G. N. G.). This research was also supported in part by the Howard Hughes Medical Institutes, William S. Smilow Center for Marfan Syndrome Research, and Center of Cancer Research (to R. I. L.). The costs of publication of this article were defrayed in part by the payment of page charges. This article must therefore be hereby marked "*advertisement*" in accordance with 18 U.S.C. Section 1734 solely to indicate this fact.

⌘ *Author's Choice*—Final version full access.

[S] The on-line version of this article (available at http://www.jbc.org) contains supplemental Figs. S1 and S2.

[1] To whom correspondence may be addressed: The Johns Hopkins University School of Medicine, 1830 E. Monument St., Rm. 547, Baltimore, MD 21205. Tel.: 443-287-3348; Fax: 410-955-0036; E-mail: eneptune@jhmi.edu.

[2] To whom correspondence may be addressed: The Johns Hopkins University School of Medicine, 733 N. Broadway, Rm. BRB539, Baltimore, MD 21205. Tel.: 410-614-0701; Fax: 410-614-2256; E-mail: hdietz@jhmi.edu.

[3] The abbreviations used are: MFS, Marfan syndrome; bHLH, basic helix-loop-helix; PNEC, pulmonary neuroendocrine cell; NEB, neuroepithelial body; PD1 and PD5, postnatal day 1 and 5, respectively; NCAM, neural cell adhesion molecule; ACTH, adrenocorticotropic hormone; CGRP, calcitonin gene-related peptide; DAPI, 4′,6-diamidinio-2-phenylindole; CgA, chromogranin A.

bellar, retinal, and inner ear development (5–7), islet cell maturation in the pancreas, and enteroendocrine cell differentiation in the small intestine (8, 9). Although targeted mice survive the neonatal period, a detailed examination of their lung phenotype has not been performed. Similarly, the role of other proneural bHLH factors (*e.g.* neurogenins and maths) in lung development is unknown.

In this study, we show that NeuroD deficiency results in impaired distal airspace formation and altered neuroendocrine cell organization. One mechanism of impaired alveolar septation in NeuroD-deficient mice is reduced airspace epithelial cell proliferation. The reduction in solitary neuroendocrine cells and increase in neuroepithelial bodies (NEBs) observed in NeuroD-deficient lung further implicate an important role for NeuroD in pulmonary neuroendocrine morphogenesis. Overexpression of NeuroD in lung epithelial cells imparts both a proliferative and neuroendocrine phenotype, suggesting a molecular link between neuroendocrine function and airspace morphogenesis. These data demonstrate cell-autonomous and cell-nonautonomous effects of NeuroD in the developing lung and illustrate the power of expression profiling analysis in the identification of determinants of complex tissue morphogenic programs.

EXPERIMENTAL PROCEDURES

Mice—Fibrillin-1-deficient mice and NeuroD-deficient mice were bred and maintained as described (1, 10). We used the NeuroD-deficient mice maintained in 129/SvJ background (11, 12). Progeny from heterozygote matings were used for the described studies. These mice were housed in a facility accredited by the American Association of Laboratory Animal Care, and the animal studies were reviewed and approved by the institutional animal care and use committee of The Johns Hopkins School of Medicine.

Expression Profiling Analysis—Lungs from fibrillin-1-deficient mice and littermate controls at postnatal day 1 (PD1) and postnatal day 5 (PD5) were harvested and quickly frozen. Lungs from two groups of mice (wild-type and fibrillin-1-deficient) at each time point were pooled in groups of two or three. Total RNA was extracted using TRIZOL reagent (Invitrogen). Expression profiling was done with Affymetrix A734 GeneChips (48 chips for this study), containing ~7000 full-length genes and ~1000 expressed sequence tags. Biotinylated cRNAs prepared from total RNAs were hybridized to U34A GeneChips in duplicate. Fluorescent signals were measured with a Hewlett Packard G2500A Gene Array Scanner. Data were analyzed with Affymetrix suite 5.0, corrected for saturation, and evaluated with GeneSpring 5.0 software. The primary gene expression data can be found on the World Wide Web at the NCBI GEO data base (GDS242).

Morphology and Histology—Three to five mice of each genotype were studied at the noted ages. For histologic and morphometric analyses, mouse lungs were inflated at 25 cm of H_2O and fixed with 4% paraformaldehyde in low melt agarose. The lungs were equilibrated in cold 4% paraformaldehyde overnight, sectioned, and then embedded in paraffin wax. Sections were cut at 5 μm and either stained with hematoxylin and eosin or processed for immunohistochemistry.

Morphometry—Measurements were performed on hematoxylin and eosin-stained sections taken at intervals throughout both lungs. Slides were coded, captured by an observer, and masked for identity. Ten to fifteen images per slide were acquired at ×20 magnification. Mean chord lengths and mean linear intercepts were assessed by automated morphometry with a macro operation performed by Metamorph Imaging Software (Universal Imaging, Molecular Devices, Downingtown, PA).

Semiquantitative PCR—Total RNAs were isolated from mouse lung by homogenization in TRIZOL reagent (Invitrogen). First-strand cDNA was prepared from 1 μg of each RNA sample using the Invitrogen Superscript II RT kit and random hexamer primers. The primers for NeuroD amplification were 5′-ATCGTCACTATTCAGAACCTT-3′ (forward) and 5′-TTCCTCGTCCTGAGAACTGAG-3′ (reverse). The primers for β-actin amplification were 5′-TTGCTGACAGGATGCAGAAG-3′ (forward) and 5′-ACATCTGCTGGAAGGTGGAC-3′ (reverse). All samples were tested in the absence of reverse transcriptase to control for DNA contamination. PCR products were analyzed on agarose gels. All results were confirmed with at least three different RNA samples.

Western Blot Analysis—Total cell lysates were extracted in M-Per buffer from Pierce. Protein concentrations were determined using the Bio-Rad Protein Assay. Aliquots of 30–50 μg of protein were boiled and then loaded onto Tris-HCl gels and transferred electrophoretically to nitrocellulose membranes. Membranes were incubated with the primary antibody for 1 h at room temperature. Detection was by the Pierce West Dura ECL detection system. Primary antibodies and dilutions were as follows: β-actin (1:1000; Abcam), c-Myc (1:1000; Abcam), NCAM (1:500; Chemicon), NCAM (DHSB (13); 1:500), ACTH (1:100; Abcam), Hes-1 (1:200; Chemicon), Mash1 (1:250; Abcam), Gfi-1 (1:250; Santa Cruz Biotechnology, Inc., Santa Cruz, CA) and chromogranin A (1:250; Santa Cruz Biotechnology).

Immunohistochemistry—Tissue sections were deparaffinized and rehydrated in an ethanol series. Sections were blocked for nonspecific binding with 3% normal serum from chicken and incubated with the primary antibodies for 1 h at room temperature. For immunofluorescence, sections were then incubated with secondary antibodies at 1:200 for 30 min at room temperature (Molecular Probes). Sections were counterstained with 4′,6-diamidinio-2-phenylindole (DAPI) and mounted with Vectashield hard set mounting medium (Vector Laboratories). For immunohistochemistry, following incubation with the primary antibody overnight at 4 °C, slides were washed with PBST, incubated with an appropriate biotinylated secondary antibody (Jackson ImmunoResearch), and developed by using ABC protocol. 5-bromo-4-chloro-3-indolyl phosphate, and 3,3′-diaminobenzidine detection reagents (Vector Laboratories). Antibodies were used at the following concentrations: NeuroD (1:100; Santa Cruz Biotechnology), PGP9.5 (1:500; Dako), synaptophysin (1:100; Zymed Laboratories Inc.), calcitonin gene-related peptide (CGRP; Sigma; 1:3000), proliferating cell nuclear antigen (1:50; Santa Cruz Biotechnology), Ki67 (1:50; Santa Cruz Biotechnology), NCAM

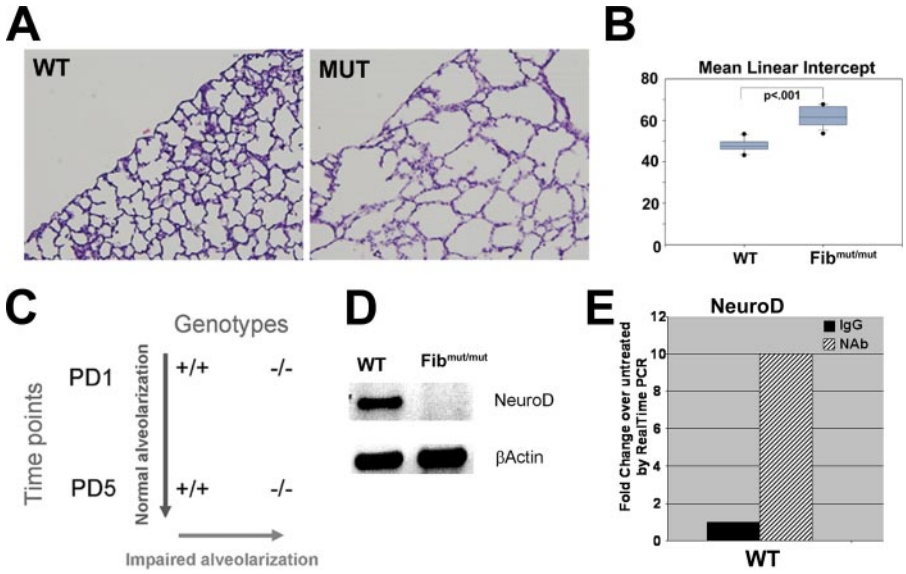

FIGURE 1. **Use of neonatal fibrillin-1-deficient mice to identify NeuroD as a candidate septation mediator.** *A*, neonatal fibrillin-1-deficient mice demonstrate enlarged airspaces (*as*). Shown are representative histologic sections of PD5 lungs stained with hematoxylin and eosin from fibrillin-1-deficient mice (*MUT*) and wild-type littermates (*WT*). *B*, morphometric assessment of airspace caliber by mean linear intercept confirms the increase in airspace caliber in the mutant mice. The figure shows significant increase in MLI in the fibrillin-1-deficient mice compared with wild-type littermates. *C*, diagram of strategy to identify candidate septation mediators by expression profile analysis. A candidate mediator was judged to have both increased expression in the PD5 wild-type lung compared with PD1 and increased expression in the wild-type PD5 lung compared with the fibrillin-1-deficient PD5 lungs. *D*, reduced NeuroD expression in fibrillin-1-deficient lung by semiquantitative PCR. *E*, real time PCR analysis of NeuroD expression in lungs from PD5 wild-type mice treated with transforming growth factor-β-neutralizing antibody demonstrated a 10-fold increase in NeuroD expression with antibody treatment. All data reflect 4–6 mice/genotype. −/−, fibrillin-1-deficient mouse.

(1:250; Chemicon), CC10 (1:1500; gift from G. Singh), TTF-1 (1:500; Dako), and active caspase-3 (1:25; Abcam).

Neuroendocrine Cell Quantitation—For details of the protocol, refer to Ref. 14. To characterize NE differentiation in fibrillin-deficient mice and wild-type littermates, we counted the total number of synaptophysin, CGRP, and PGP9.5 immunoreactive solitary PNECs and NEBs (neuroendocrine foci) in formaldehyde-fixed, paraffin-embedded lung sections. This was correlated to the number of airways in the same sections (foci/airway). To determine the size of NEBs in these same mice, pictures of each NEB were acquired using MetaMorph® software (Universal Imaging/Molecular Devices, Downingtown, PA). The immunoreactive area was manually outlined and measured using the same software, and the size in μm^2 for each individual NEB was tabulated. Statistical analysis was performed using the Mann-Whitney test (SigmaStat).

For differential measurement of solitary PNECs *versus* NEBs, lung tissue sections were co-stained with PGP9.5 (Dako) and DAPI (Molecular Probes) as described under "Immunohistochemistry." The total number of airway cells was determined by counting cells per 20× field staining positive for DAPI in the airway. Neuroendocrine cells were quantified based on the total number of cells staining positive for PGP9.5. Those cells positive for PGP9.5 were characterized as either components of NEBs (cluster of ≥3 neuroendocrine cells) or solitary neuroendocrine cells based on morphology. These two neuroendocrine cell types were then quantified and normalized to airway basement membrane length in $\mu m \times 10^4$.

Cell Culture and Transfection—The MLE12 cell line, an immortalized mouse lung epithelial cell line that maintains characteristics of type II alveolar epithelial cells (15), was a kind gift from Dr. Jeffrey Whitsett (University of Cincinnati) and was maintained in Dulbecco's minimal essential medium/F-12 medium (1:1) supplemented with 2% fetal calf serum. Subconfluent cells were transfected with Lipofectamine Plus (Invitrogen) according to the manufacturer's protocol and harvested after 24 or 48 h. All transfections were performed in triplicate. The Myc-tagged murine NeuroD cDNA construct was a gift from Drs. David Turner (University of Michigan) and Jacqueline Lee (University of Colorado).

For conditioned media experiments, medium was removed from transiently transfected cells after 24 h and replaced with serum-free medium. Supernatants were harvested after 24 and 48 h, and cells were removed by low speed centrifugation. After washing with phosphate-buffered saline, serum-starved MLE12 cells were treated with supernatants from transfected cells. For proliferation assays, cells were incubated for the designated time periods after treatment or transfection and then assayed per protocol with the Promega CellTitre 96 nonradioactive proliferation assay.

Data Analysis—Absolute analysis of Affymetrix image data were done using Affymetrix Microarray Suite 4.0. Values of intensity differences as well as ratios of each probe pair are used for determination of whether a transcript is called "present" or "absent." The differentially expressed gene lists for each time point were generated using GeneSpring software (Silicon Genetics, CA). In GeneSpring, those genes showing at least four Affymetrix present calls were selected prior to further data processing. Welch's *t* test was performed to calculate the probabilities of significant gene expression changes. Since the probe sets were tested multiple times, we used a highly stringent *p* value cut-off ($p < 0.001$) to reduce the number of false positives to less than 1 in 1000.

Statistical Analysis—Analysis of variance and Student's *t*-tests were used to determine differences between groups. In the morphometric study, statistical differences were determined by the unpaired Student's *t* test for comparison of septal measurements. Values for all measurements were expressed as means ± S.E., and *p* values for significance were designated at <0.05.

RESULTS

Fibrillin-1 Deficiency Is Associated with Airspace Defects and Reduced Expression of NeuroD—Neonatal mice deficient in fibrillin-1 display increased airspace caliber at PD5, a time point that coincides with the initiation of alveolar septation in the

murine lung (Fig. 1, *A* and *B*). In order to identify candidate mediators of distal lung development, whole organ gene expression profiling was performed on wild-type and fibrillin-1-deficient mice at PD1 and PD5. Upon pairwise comparison, we reasoned that candidate genes would be (*a*) down-regulated in the mutant lung compared with wild-type lung on PD5 and (*b*) increased in the wild-type PD5 lung compared with the wild-type PD1 lung (Fig. 1*C*). Interestingly, NeuroD, a basic helix-loop-helix protein, demonstrated a 25-fold induction in the wild-type PD5 lung compared with the wild-type PD1 lung and a 5-fold reduction in the fibrillin-1 PD5 lung compared with wild-type littermates. These results were confirmed by semiquantitative RT-PCR (Fig. 1*D*). Since transforming growth factor-β-neutralizing antibody restores normal septation in fibrillin-deficient mice, we determined whether NeuroD levels responded to this maneuver. We found a 10-fold induction of NeuroD expression in the wild-type lung upon treatment with antibody treatment but only a 1.5-fold induction in the mutant lung. This finding suggests that although NeuroD deficiency may contribute in a minor way to the lung phenotype in the fibrillin-1-deficient mouse, it is not a predominant mechanism. Since fibrillin-1 deficiency is associated with complex disturbances involving tissue structure, cytokine dysregulation, and recently angiotensin signaling, the lack of an intimate mechanistic association between NeuroD signaling and the fibrillin-1 phenotype is not unexpected (1, 16–19). Nonetheless, we surmised, NeuroD might play a role in lung maturation distinct from the context of fibrillin-1 deficiency.

NeuroD-deficient Mice Have Impaired Alveolar Formation Secondary to Reduced Airspace Epithelial Proliferation—Our expression profiling strategy was designed to identify determinants of distal lung formation. In order to establish whether NeuroD is critically involved in distal lung morphogenesis, we examined the lung phenotype of mice deficient in NeuroD. These mice had known defects in pancreatic, enteroendocrine, cerebellar, and hippocampal morphogenesis, but their lung phenotype has not been examined. The homozygous mutant mice had a marked increase in distal airspace caliber at PD5 and PD10 compared with littermate controls, similar to our findings in fibrillin-1-deficient mice (Fig. 2, *A* and *B*). By adulthood, the airspace caliber remained significantly larger than the wild type controls but showed no progression compared with the PD10 mutant lung. Using markers of alveolar epithelial cells (TTF-1) and airway epithelial cells (CC10), we found preserved epithelial differentiation in the neonatal mutant lung (Fig. 2, *C* and *D*). Since airspace simplification can result from reduced proliferation or increased cell death in the lung parenchyma, we examined distal lung proliferation and apoptosis in the developing and adult lungs. We found a dramatic reduction (27%) in proliferation of airway and alveolar epithelial cells in the developing airspace and airway of the mutant lung (Fig. 3, *A* and *B*) but no difference in apoptosis by terminal dUTP nick-end labeling and active caspase 3 staining (data not shown). This profile contrasts with our finding of increased apoptosis but normal proliferation in fibrillin-1-deficient murine lungs. Importantly, the mitotic index falls to trivial levels in the mutant and wild-type lung by adulthood (Fig. 3*B*) and is probably responsible for the inability to correct the airspace enlargement after lung maturation. Taken together, these data suggest that the early airspace phenotype of these mice is not attributable to an altered epithelial differentiation program but rather to reduced epithelial proliferation.

NeuroD-deficient mice in the Sv/129 background have ~30–40% perinatal mortality, strictly observed within the first week of life (12). Between the time points of PD5 and adulthood, we observed no mutant pup loss. Since PD10 is beyond the point of expected pup loss but still within the terminal phase of lung alveolar development, our demonstration of persistent airspace enlargement suggests that the PD5 phenotype did not merely reflect mice that would ultimately die before adulthood (Fig. 2, *A* and *B*). However, in order to further establish that the PD5 and PD10 mice were comparable, we evaluated Mendelian ratios of respective genotypes. Assessment of 40+ mice at each time point revealed 26, 52, and 22% *versus* 23, 57, and 20% ($NeuroD^{+/+}$, $NeuroD^{+/-}$, and $NeuroD^{-/-}$ genotypes), respectively, at PD5 and PD10. We also found no reduction in weight in the mutant mice at either PD5 or PD10, suggesting that mice assessed at these two time points were comparable (see supplemental materials).

NeuroD Is Expressed in Pulmonary Neuroendocrine Cells, and Fibrillin-1-deficient Mice Have Altered Neuroendocrine Cell Morphology—Mice with a targeted deletion in Mash1, another proneural bHLH factor, do not develop pulmonary neuroendocrine cells and die in the neonatal period (20). Because neuroendocrine cells probably perform an endocrine function for the developing lung by secreting growth factors that are instructive for distal lung morphogenesis (10, 11), we considered whether NeuroD might be involved in neuroendocrine cell differentiation and function (21, 22). We used the panneuroendocrine marker PGP9.5 to assess the morphology and abundance of neuroendocrine cells. Immunohistochemical studies employing antibodies against NeuroD and PGP9.5 revealed that NeuroD is expressed in pulmonary neuroendocrine cells within the distal airway (Fig. 4*A*). To explore the possibility that the reduction in NeuroD expression in the fibrillin-1-deficient lung was secondary to an abnormality in the neuroendocrine compartment, we examined the quotient of neuroendocrine cells in fibrillin-1-deficient lungs. We have previously reported that reduced neuroendocrine cell number and/or mass area correlate with altered neuroendocrine maturation (14). The total number of neuroendocrine foci (composed of NEBs and PNECs) was significantly higher in PD5 fibrillin-deficient mice compared with wild-type littermates (Fig. 4*B*). However, the average size of NEBs in fibrillin-deficient animals was about 30% smaller than that in control mice ($p = 0.056$) (Fig. 4*C*). Thus, although there was a modest increase in neuroendocrine foci in the fibrillin-1-deficient lung (Fig. 4*B*), we found a trend toward reduction in the size of NEBs in the NeuroD mutant lung (Fig. 4*C*), consistent with impaired neuroendocrine maturation.

NeuroD-deficient Mice Have an Alteration in Pulmonary Neuroendocrine Morphology—Given that inactivation of the proneural bHLH factor Mash1 prevents pulmonary neuroendocrine differentiation (20), we hypothesized that a similar impairment might exist in NeuroD-deficient mice. Surprisingly, we found that neuroendocrine cells were present

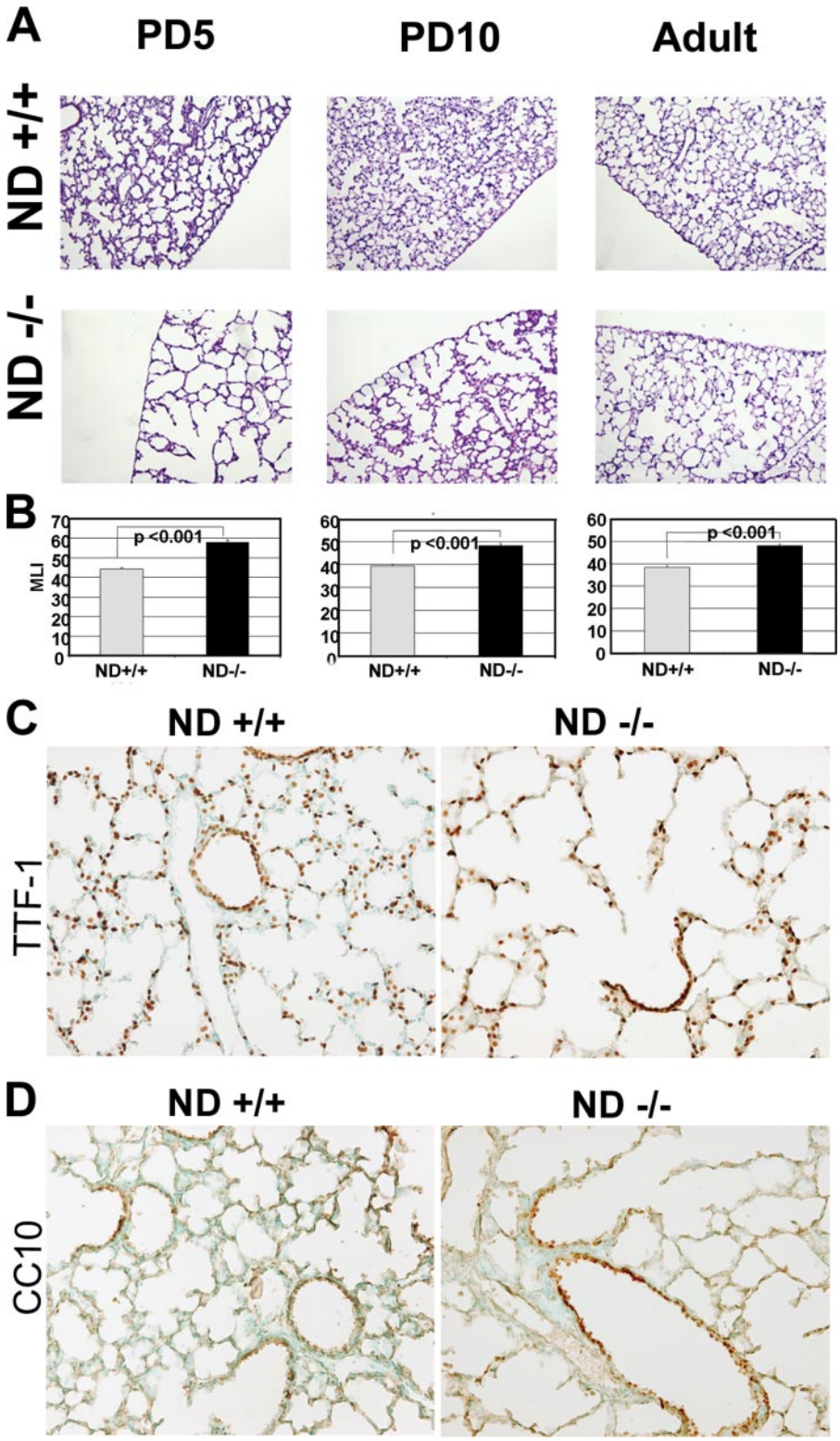

FIGURE 2. **NeuroD-deficient mice have increased airspace caliber reminiscent of fibrillin-1-deficient mice and preserved lung epithelial differentiation.** *A*, representative histology of lungs from PD5, PD10, and 6-week-old wild type and NeuroD-deficient mice demonstrates a marked increase in airspace caliber in the neonatal mutant lung. Lungs were inflated at constant pressure, fixed, sectioned, and stained with hematoxylin and eosin. *B*, morphometric analysis confirms the significant increase in airspace size in the NeuroD-deficient lung using parameters of mean linear intercept (*MLI*) in μm. *, $p < 0.01$. *C*, immunostaining of PD5 WT and NeuroD-deficient lungs for TTF-1, a marker of distal bronchiolar and type II alveolar epithelial cells, shows preserved differentiation in the mutant lung. *D*, immunostaining of PD5 WT and NeuroD-deficient lungs for CC10, a marker of nonciliated airway epithelial cells shows preserved differentiation in the mutant lung. All data reflect 4–6 mice/genotype. *ND* +/+, control wild-type littermate; *ND* −/−, NeuroD-deficient mouse.

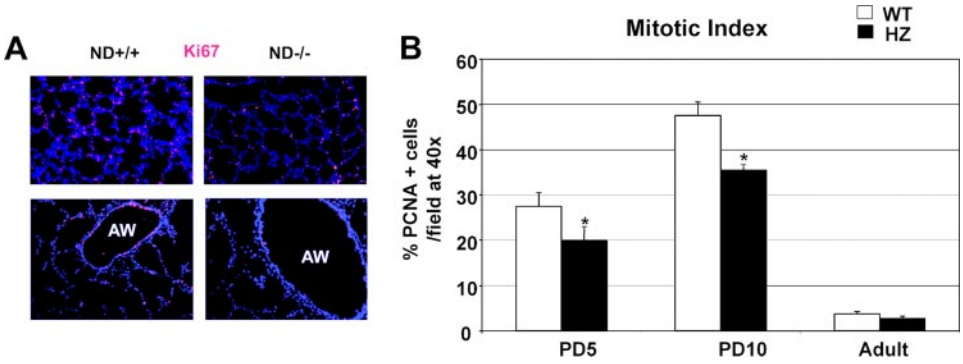

FIGURE 3. **NeuroD-deficient lungs have reduced proliferation in airspace and airway compartments.** *A*, the proliferative status of the wild-type and mutant PD5 lung was assessed by immunohistochemistry for Ki67, a proliferation marker. *Top*, lung parenchyma of representative wild-type and mutant mice. *Bottom*, airway compartment of representative wild-type and mutant mice. *Red*, Ki67; *blue*, DAPI. *B*, mitotic index of parenchymal cells in NeuroD-deficient and wild-type lungs at three different time points shows a significant reduction in proliferation in the mutant lung during the neonatal period. Lungs were stained for PCNA, another marker of proliferation. Positive cellular staining in the airspace and airway were normalized for total cell count as measured by DAPI immunofluorescence to generate a mitotic index. *, $p < 0.001$. *ND +/+*, control wild-type littermate; *ND −/−*, NeuroD-deficient mouse.

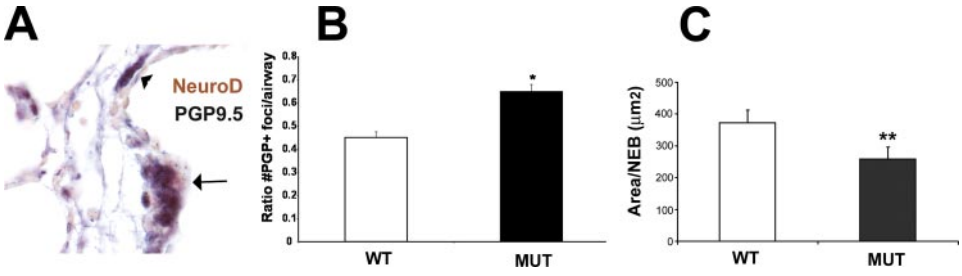

FIGURE 4. **NeuroD is expressed in NEBs in the developing lung, and fibrillin-1-deficient mice have abnormal neuroendocrine system morphology.** *A*, dual immunohistochemistry of PD5 wild type lung demonstrates colocalization of NeuroD and PGP9.5, a neuroendocrine marker. The *arrow* denotes a nerve fiber accompanying the NEB. *Red*, NeuroD; *black*, PGP9.5. *B*, fibrillin-1-deficient mice have slightly increased neuroendocrine cell number compared with littermate controls. PD5 lungs from wild-type and fibrillin-1-deficient mice were stained with PGP9.5. Positively stained foci were counted and normalized to airway number in a given specimen. *C*, fibrillin-1-deficient mice have a trend toward reduced neuroendocrine cell mass compared with littermate controls. Total area of NEBs (identified by the aforementioned marker) was measured in each lung specimen to generate a mean area per NEB. This parameter reflects NEB maturation. All data reflect 4–6 mice/genotype. *, $p = 0.013$; **, $p = 0.056$, *WT*, wild type; *MUT*, fibrillin-1-deficient.

throughout airway and airspace development in the mutant lung (Fig. 5*A*). Pulmonary neuroendocrine cells exist in two distinct morphologies: solitary PNECs and NEBs. The former subserves a primary secretory function, liberating mitogenic and vasoactive amines, and the latter is thought to act as a hypoxia and/or chemoreceptor (23, 24). When we quantified the number of solitary PNECs *versus* NEBs in NeuroD-deficient mice, we found (*a*) a significant increase in the number of NEBs in the mutant lung, similar to the fibrillin-1 deficient lung, but (*b*) a striking reduction in solitary PNECs in the mutant lung (Fig. 5, *B–D*). Neuroendocrine hyperplasia attends several inflammatory and fibrotic lung disorders, such as bronchopulmonary dysplasia and cystic fibrosis, and is thought to contribute to these conditions via the liberation of profibrotic cytokines. Because solitary PNECs are thought to function primarily as endocrine cells without neural innervation, we considered whether the marked reduction in the number of these cells correlated with impaired liberation of mitogenic amines and reduced distal airspace cell proliferation.

To determine whether the time course of the altered neuroendocrine morphology correlated with the evolution of airspace lesion, we quantified neuroendocrine cells during murine lung development (PD5 and PD10) and early adulthood (6 weeks). We found a persistent increase in NEBs and reduction in solitary PNECs during the first 2 weeks of postnatal life but a full normalization by adulthood (Fig. 5, *E* and *F*). Thus, by temporal criteria, the altered neuroendocrine morphology may partially contribute to the airspace lesion, plausibly via suboptimal liberation of mitogenic amines by solitary PNECs.

Since NeuroD-deficient mice were maintained in the Sv/129 strain but the fibrillin-1-deficient mice were maintained in a mixed Sv/129:C57Bl/6 background, we wanted to establish that the baseline relative neuroendocrine profile was comparable in these two strains. We quantified solitary PNECs, NEBs, and total neuroendocrine cells in PD5 mice of each background strain and found a reduced proportion of NEBs in both strains (18 ± 5% NEB/PNEC ratio in Sv/129 strain and 30 ± 2% in Sv/129/C57Bl/6 background). Accordingly, the reversal of this ratio in the NeuroD-deficient mice has broad relevance to both background strains.

NeuroD Overexpression Confers a Neuroendocrine Phenotype—NeuroD family members promote progenitor cell differentiation in neural and endocrine tissues. Although neuroendocrine cells are present in the primitive vertebrate lung, their resident precursor has not been identified. Notably, lineage tracing of surfactant protein C-expressing (SPC^+) progenitors in the developing murine lung did not demonstrate $CGRP^+$ neuroendocrine progeny in the perinatal period (25). By contrast, Wuenschell *et al.* (26) characterized a pluripotent cell type in the developing lung that expressed neuroendocrine, airway, and alveolar epithelial markers, suggesting that a common precursor might exist. In order to determine whether the overexpression of NeuroD in a nonneuroendocrine-derived cell line was sufficient to induce the neuroendocrine phenotype, we overexpressed a Myc-tagged NeuroD in a nonneuroendocrine mouse lung alveolar epithelial cell line (MLE12). Remarkably, NeuroD expression induced robust expression of chromogranin A and ACTH, both neuroendocrine markers and p21 expression (Fig. 6*A*). We did not find repression of surfactant protein B or TTF-1, markers of lung epithelial cells (data not shown). Furthermore, using two different antibodies for NCAM detection, we found that NeuroD expression induced high molecular weight NCAM140 expression (Fig. 6*B*). Since Ito described opposing effects of

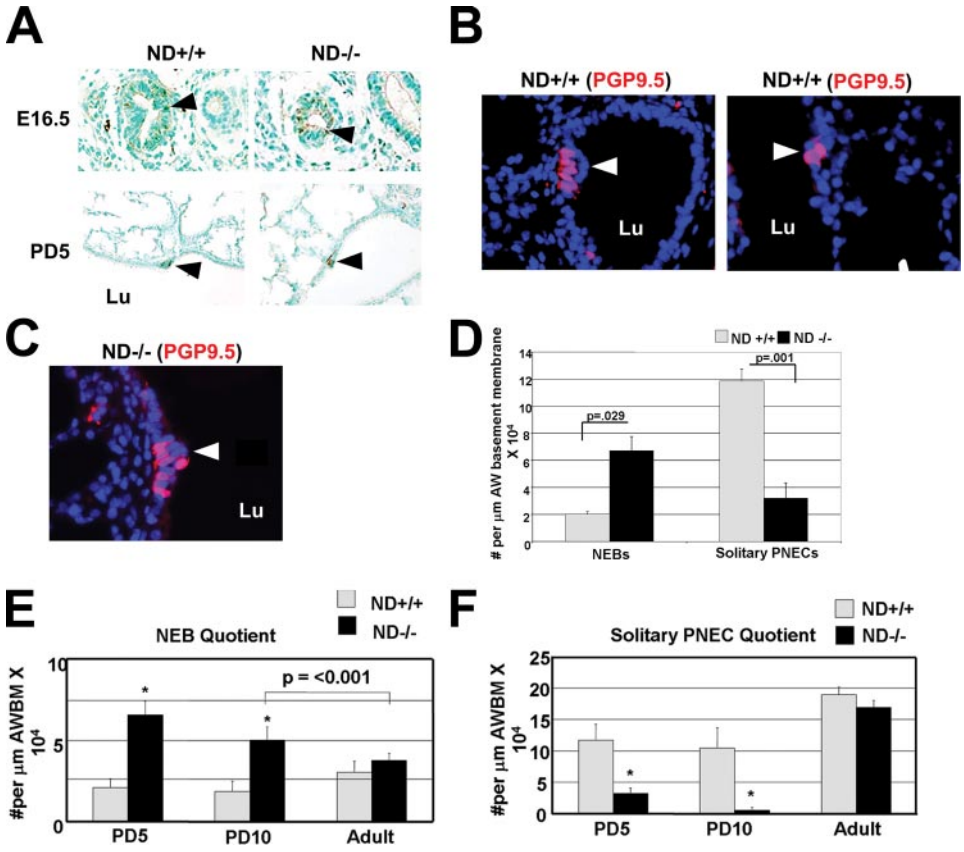

FIGURE 5. **NeuroD-deficient mice demonstrate abnormal neuroendocrine cell compartment morphology.** *A*, NeuroD-deficient murine lungs at embryonic day 16.5 and PD5 demonstrate NEBs within the airways. The *arrowheads* denote sites of PGP9.5 staining within the distal airway. *B*, wild-type PD5 lungs have both NEBs (*arrow*, *left*) and solitary pulmonary neuroendocrine cells (PNECs) (*arrow*, *right*). Representative sections from wild type (*WT*) and NeuroD-deficient lungs stained for PGP9.5 (*red*), a marker of neuroendocrine cells. Total cell nuclei are represented by DAPI staining (*blue*). NEBs are defined as a cluster of ≥3 PNECs. *C*, PD5 NeuroD-deficient lungs have neuroepithelial cell bodies but rare solitary PNECs. Neuroendocrine cells in NeuroD-deficient lungs stained for PGP9.5 are primarily in an NEB conformation. The *arrowhead* denotes representative NEB present in a NeuroD-deficient lung. *D*, quantitation of NEBs and solitary PNECs in airways of NeuroD-deficient mice and wild-type littermates shows a significant increase in NEBs associated with a marked reduction in solitary PNECs per airway length in the mutant lung. Lungs from respective mice were stained for PGP9.5 as described above. NEBs and PNECs were counted in 15 low power fields and normalized to total airway perimeter in fields. *E*, quantification of NEBs normalized to airway basement membrane (*AWBM*) length at three different time points demonstrates a persistent increase in these structures in the mutant lung during the first 2 weeks of life compared with wild-type littermates but normalization by adulthood. *, $p < 0.001$. *F*, quantification of solitary PNECs per airway basement membrane length at three different time points demonstrates a marked reduction in these cells in the mutant lung during the first 2 weeks of life compared with wild-type littermates but normalization by adulthood. *, $p < 0.001$. *Arrowheads*, NEBs and neuroendocrine cells. *Arrows*, proliferating epithelia. All data reflect 4–6 mice/genotype. *Lu*, lumen; *AW*, airway.

Mash1 and Hes-1 in neuroendocrine maturation, we surveyed both of these candidate mediators after NeuroD overexpression (27). Although we observed no change in the levels of Hes-1, we did see an induction of Mash1 at 24 h, consistent with its critical early role in neuroendocrine differentiation (Fig. S2). We also observed an induction of Gfi-1, a recently identified neuroendocrine determinant, in NeuroD-overexpressing cells (28). In summary, the whole cell studies suggest that NeuroD overexpression is sufficient to confer a neuroendocrine phenotype to lung epithelial cells.

NeuroD Overexpression Induces Autocrine and Paracrine Proliferation in Lung Epithelial Cells—Although they represent a relatively sparse cell population in the lung, neuroendocrine cells can alter geographic proliferative and morphogenic programs via autocrine and paracine effects on local epithelial cells. Notably, we have recently shown that mice that are deficient in Gfi1, a determinant of neuroendocrine cell morphogenesis, display reduced airway cell proliferation after naphthalene injury (29). In order to connect the altered neuroendocrine developmental phenotype we observed in NeuroD deficient lungs with reduced epithelial proliferation, we examined whether overexpression of NeuroD in lung epithelial cells increased proliferation. We found a significant increase in proliferation in cells transfected with NeuroD compared with cells transfected with a control vector (Fig. 7*A*). Since we observed reduced proliferation in cells that did not express NeuroD in the airway and epithelium of the distal lung, we examined whether NeuroD-transfected cells secreted mitogenic factors (a known property of neuroendocrine cells) that induced proliferation in cells not expressing NeuroD. Conditioned medium from cells transfected with NeuroD promoted a >55% increase in proliferation compared with medium from vector-transfected cells (Fig. 7*B*). These data suggest that NeuroD expression supports autocrine and paracrine proliferative signaling in lung epithelial cells. This mechanism may account for the widespread reduction in proliferation in the NeuroD-deficient lung.

DISCUSSION

Although neuroendocrine cells represent less than 1% of epithelial cells in the vertebrate lung, they are active participants in lung repair and malignant transformation (reviewed in Ref. 30). Consistent with previous reports of NeuroD expression in neuroendocrine tumors (31), we show here that NeuroD is expressed in the neuroendocrine cells of the developing lung. We also describe for the first time a temporal association between the maturation of the pulmonary neuroendocrine compartment and distal lung morphogenesis. Reminiscent of its role in the gastrointestinal tract and the pancreas, one of the pulmonary effects of NeuroD deficiency is an alteration in the morphology of the pulmonary neuroendocrine compartment. However, it follows that for these relatively sparse PNECs to participate in global morphogenic functions, paracrine effects mediated by secreted factors must be operative. We show here that a disturbance in PNEC morphology conferred by a deficiency in NeuroD may contribute to a more global morphogenic pertur-

bation. Several investigators have shown that mitogens (bombesin-like peptides, gastrin-releasing peptide, CGRP, etc.) synthesized and secreted by PNECs induce airway and alveolar epithelial cell proliferation in explant and whole cell systems (32–34). Sunday *et al.* (35) have also demonstrated adverse effects of exaggerated pulmonary neuropeptide secretion in the neonatal setting, possibly contributing to bronchopulmonary dysplasia and other lung diseases of prematurity. Cutz and co-workers (36) have shown that the lung parenchymal phenotype of cystic fibrosis transmembrane conductance regulator-deficient mice includes disturbances in PNEC and NEB morphogenesis. Taken together, the mitogenic and morphogenic consequences of PNEC dysregulation probably contribute to parenchymal lung disease. However, because of the paucity of reagents that alter local neuropeptide secretion and function in the lung, a direct confirmation of the *in vivo* consequences of altered neuroendocrine system morphology has yet to be provided.

The pulmonary phenotype of NeuroD-targeted mice recapitulates selective aspects of the nonneuronal phenotypes observed in other organs. In the small intestine and pancreas, NeuroD deficiency promotes cell autonomous apoptotic cell loss and reduced proliferation. In this report, although we show compromised proliferation, we do not detect enhanced apoptosis in the lung parenchyma of mutant mice. However, we cannot rule out the possibility that apoptotic loss of PNECs precedes the observed antiproliferative phenotype.

Despite the fact that NEBs and solitary PNECs are highly conserved phylogenetically, the physiological significance and the developmental ontogeny of these two morphologies remain unclear (37). Additionally, the genetic and biochemical pathways that instruct neuroendocrine differentiation are unknown. Apart from the complete absence of pulmonary neuroendocrine cells in Mash1-deficient mice, no published genetically targeted model has shown alterations of neuroendocrine morphology using the most PNEC-inclusive marker, PGP9.5. Mice deficient for Gfi-1 have reduced CGRP-expressing solitary PNECs and NEBs but preserved abundance of PGP9.5-expressing cells (28). The combination of a marked reduction in solitary PNECs and expansion in NEBs that we show in the NeuroD-deficient lung supports integrative developmental regulation of these two structures. Two models reconcile this dual compartment mechanism. First, solitary PNECs may originate in the NEB niche, but at an early developmental time point, separate from the cluster. Accordingly, it remains possible that the lack of solitary PNECs in the NeuroD-deficient lung reflects an as yet undefined defect in the NEB niche. A second model is that solitary PNECs and NEBs may have a common resident precursor but develop as distinct, nonoverlapping entities, with only the former requiring NeuroD expression for terminal differentiation. The development of methods to reliably isolate these low abundance cells from rodent lungs would greatly facilitate our dissection of their differentiation programs.

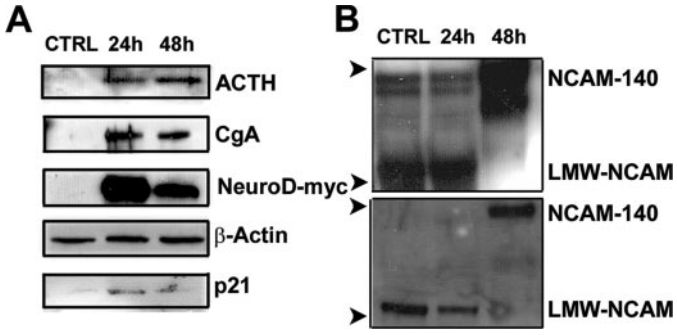

FIGURE 6. **NeuroD overexpression in lung epithelial cells induces a neuroendocrine phenotype.** *A*, NeuroD expression in a lung epithelial cell line induces ACTH, chromogranin A, and p21. Lysates from MLE12 cells transiently overexpressing NeuroD-Myc or plasmid control were subjected to immunoblotting for ACTH, chromogranin A, and p21. The same membrane was probed with an anti-β-actin antibody to assess equal loading of the gel and an anti-c-Myc antibody to document the overexpression of NeuroD. *B*, NeuroD overexpression induces expression of NCAM1, a marker of mature neuroendocrine cells. Membranes of lysates from MLE12 cells transfected with NeuroD-Myc were immunoblotted for NCAM1 using both polyclonal antibody AB5032 (Chemicon) (*top*) and polyclonal antibody AG1 (DSHB) (*bottom*). The *arrowheads* denote position of low molecular mass (~75 kDa) and high molecular mass (>150 kDa) NCAM. The blots are representative of >3 experiments. *24h*, 24 h after transfection; *48h*, 48 h after transfection. *LMW-NCAM*, low molecular weight, nonmodified NCAM.

The finding of impaired alveolar septation in the NeuroD-deficient lung seems discordant, given that NeuroD is not expressed in the airspace. The markedly reduced airway and airspace proliferation implicate a global perturbation in mitogenesis. Two mechanisms are plausible. First, since neuroendocrine cells liberate mitogenic amines that act in a local paracrine manner and which are known to be involved in lung morphogenesis, the reduced solitary neuroendocrine cell compartment might compromise the liberation of requisite promorphogenic factors during alveolar development. Our finding of NeuroD-induced proliferation in transfected MLE12 cells supports this mechanism. Second, the known diabetic

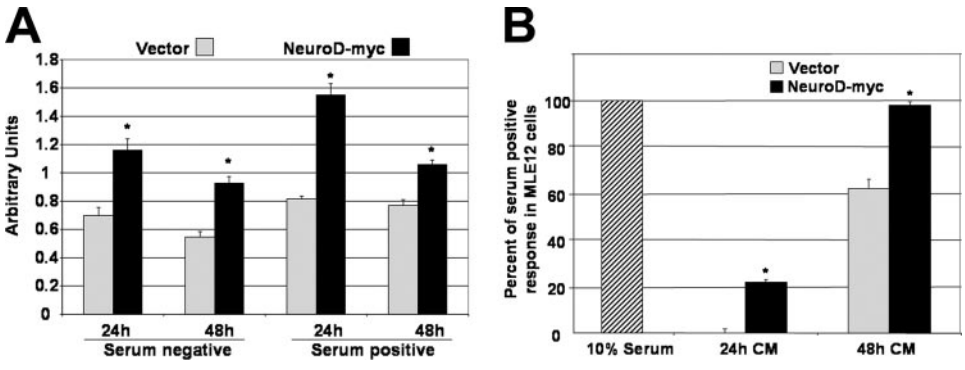

FIGURE 7. **NeuroD overexpression enhances proliferation in an autocrine and paracrine manner.** *A*, MLE12 cells transfected with NeuroD display increased proliferation. Cells transfected with either NeuroD-Myc or pci-Neo (*Vector*) were evaluated after 24 and 48 h for proliferation, as measured by the CellTitre96 nonradioactive proliferation assay (Promega). *B*, conditioned medium from NeuroD-Myc or transfected cells promote increased proliferation of MLE12 cells. Supernatants from cells transfected with NeuroD-Myc or pci-Neo were filtered and then added to subconfluent MLE12 as a 1:1 dilution with serum-free medium. Proliferation was measured after 24 and 48 h as described above. All experiments were performed in triplicate. *, $p < 0.05$.

phenotype of these mice could exert antimorphogenic effects on the lung, an interaction that has been observed in human and animal models (38, 39). Although the precise basis for the airspace phenotype is unclear, the finding supports an intimate interaction between lung morphogenesis and overall neuroendocrine function.

Our induction of neuroendocrine marker expression in murine lung epithelial cells suggests that NeuroD expression is sufficient to confer a neuroendocrine phenotype. Leiter and co-workers (8) showed that NeuroD expression in HeLa cells promoted the expression of p21 and secretin. NeuroD overexpression in non-islet-derived pancreatic cell lines triggered a beta cell differentiation program exemplified by NKX2.2, pax4, and insulin induction (40, 41). Our results demonstrate that nonneuroendocrine lung epithelial cells harbor the requisite machinery to drive differentiation into neuroendocrine cells upon overexpression of NeuroD. We observed that NeuroD induced a restricted repertoire of neuroendocrine markers. Therefore, multiple transcription factors may be required for the expression of the full repertoire of panneuroendocrine markers in a given lung epithelial cell. Alternatively, a given bHLH protein may activate the differentiation of a restricted subset of pulmonary neuroendocrine cells that express a defined repertoire of markers, a pattern observed in the enteroendocrine compartment (42, 43). Ito *et al.* (27) demonstrated that NeuroD expression in the postnatal lung temporally coincided with Mash1 mediated neuroendocrine cell differentiation, suggesting some measure of cooperativity among these proneural factors.

Lung alveolarization is a dynamic and highly regulated process that integrates proliferative, apoptotic, and morphogenic cues. Both fibrillin-1 deficiency and NeuroD deficiency show impaired alveolar septation in the immediate postnatal period. However, meaningful differences in these phenotypes are evident. In fibrillin-1-deficient mice, the airspace lesion is progressive throughout postnatal life, whereas in the NeuroD-deficient lung, the airspace lesion improves but does not fully correct over time. These findings suggest that NeuroD may participate in the onset of alveolar septation but not the maintenance of the airspace architecture. By contrast, fibrillin-1 deficiency, in affecting the structural integrity of the airspace as well as the cytokine milieu, affects both the establishment and the maintenance of airspace architecture (1, 17, 19, 44). We reported that not only does fibrillin-1 deficiency compromise airspace formation and maintenance, but it also contributes to late onset inflammatory emphysema that recapitulates acquired airspace enlargement. Simply stated, isolated NeuroD deficiency *versus* relative NeuroD deficiency in the context of fibrillin-1 deficiency leads to distinct airspace sequelae. In this view, our data suggest that NeuroD deficiency is not the sole or predominant determinant of the airspace enlargement observed in fibrillin-1-deficient mice; rather, primary structural distortions and secondary alterations in cytokines are the critical determinants of the more severe and sustained lesion evident in these mice.

There are significant differences between the lung phenotypes of the fibrillin-1-deficient and the NeuroD-deficient mice. First, the airspace defect in the fibrillin-1-deficient mice is attributable to enhanced apoptosis conferred by increased transforming growth factor-β signaling. By contrast, the airspace defect in the NeuroD-deficient mice is a result of reduced proliferation. Second, the airspace lesion in fibrillin-1-deficient mice is progressive, whereas the airspace phenotype in the NeuroD-deficient mice remains stable throughout early adulthood, suggesting that the critical insult occurs during a discrete phase of development without ongoing perturbations. Thus, the down-regulation of NeuroD in fibrillin-1-deficient mice might well be a secondary effect of altered lung maturation and not specifically referable to fibrillin-1 biology.

We conclude that NeuroD, a proneural bHLH factor, contributes to early airway and airspace homeostasis. In the airspace, NeuroD must utilize cell nonautonomous pathways to maintain the proliferative milieu required for normal alveolar morphogenesis. Similarly, dysregulated expression of NeuroD may contribute to pathologic proliferation, as is observed in lung malignancies that overexpress NeuroD (31). In keeping with this previously unrecognized capacity, we report increased proliferation in alveolar epithelial cells overexpressing NeuroD and in epithelial cells exposed to supernatants from NeuroD expressing cells. In the airway, NeuroD is a primary determinant of NE morphology, facilitating the generation of solitary PNECs plausibly from preexistent NEBs. Since one or both of these morphologies may be the cellular substrate for the development of neuroendocrine-type lung malignancies, a better understanding of the specific contextual functions of these cells is needed.

Acknowledgments—We thank Keri Pearson and Eric Hoffman (Children's National Medical Center, Washington D. C.) for help with the microarray assays. We thank Dr. Xu Naizhen for immunohistochemical staining and morphometric analyses. We thank Sylvia McCay and Kimberly Gordy for technical assistance. We thank Douglas Ball, Ari Zaiman, Mark Awad, Neda Sharifi, and other members of the Dietz and Tuder laboratories for critical reading of the manuscript and helpful advice.

REFERENCES

1. Neptune, E. R., Frischmeyer, P. A., Arking, D. E., Myers, L., Bunton, T. E., Gayraud, B., Ramirez, F., Sakai, L. Y., and Dietz, H. C. (2003) *Nat. Genet.* **33,** 407–411
2. Bertrand, N., Castro, D. S., and Guillemot, F. (2002) *Nat. Rev. Neurosci.* **3,** 517–530
3. Chu, K., Nemoz-Gaillard, E., and Tsai, M. J. (2001) *Recent Prog. Horm. Res.* **56,** 23–46
4. Ball, D. W. (2004) *Cancer Lett.* **204,** 159–169
5. Morrow, E. M., Furukawa, T., Lee, J. E., and Cepko, C. L. (1999) *Development* **126,** 23–36
6. Miyata, T., Maeda, T., and Lee, J. E. (1999) *Genes Dev.* **13,** 1647–1652
7. Kim, W. Y., Fritzsch, B., Serls, A., Bakel, L. A., Huang, E. J., Reichardt, L. F., Barth, D. S., and Lee, J. E. (2001) *Development* **128,** 417–426
8. Mutoh, H., Fung, B. P., Naya, F. J., Tsai, M. J., Nishitani, J., and Leiter, A. B. (1997) *Proc. Natl. Acad. Sci. U. S. A.* **94,** 3560–3564
9. Naya, F. J., Huang, H. P., Qiu, Y., Mutoh, H., DeMayo, F. J., Leiter, A. B., and Tsai, M. J. (1997) *Genes Dev.* **11,** 2323–2334
10. Pereira, L., Andrikopoulos, K., Tian, J., Lee, S. Y., Keene, D. R., Ono, R., Reinhardt, D. P., Sakai, L. Y., Biery, N. J., Bunton, T., Dietz, H. C., and Ramirez, F. (1997) *Nat. Genet.* **17,** 218–222
11. Cho, J. H., and Tsai, M. J. (2006) *Dev. Biol.* **290,** 125–138
12. Liu, M., Pleasure, S. J., Collins, A. E., Noebels, J. L., Naya, F. J., Tsai, M. J., and Lowenstein, D. H. (2000) *Proc. Natl. Acad. Sci. U. S. A.* **97,** 865–870

13. DiFiglia, M., Marshall, P., Covault, J., and Yamamoto, M. (1989) *J. Neurosci.* **9,** 4158–4168
14. Castro, C. M., Yang, Y., Zhang, Z., and Linnoila, R. I. (2000) *Lab. Invest.* **80,** 1533–1540
15. Yei, S., Bachurski, C. J., Weaver, T. E., Wert, S. E., Trapnell, B. C., and Whitsett, J. A. (1994) *Am. J. Respir. Cell Mol. Biol.* **11,** 329–336
16. Carta, L., Pereira, L., Arteaga-Solis, E., Lee-Arteaga, S. Y., Lenart, B., Starcher, B., Merkel, C. A., Sukoyan, M., Kerkis, A., Hazeki, N., Keene, D. R., Sakai, L. Y., and Ramirez, F. (2006) *J. Biol. Chem.* **281,** 8016–8023
17. Cohn, R. D., van Erp, C., Habashi, J. P., Soleimani, A. A., Klein, E. C., Lisi, M. T., Gamradt, M., ap Rhys, C. M., Holm, T. M., Loeys, B. L., Ramirez, F., Judge, D. P., Ward, C. W., and Dietz, H. C. (2007) *Nat. Med.* **13,** 204–210
18. Judge, D. P., Biery, N. J., Keene, D. R., Geubtner, J., Myers, L., Huso, D. L., Sakai, L. Y., and Dietz, H. C. (2004) *J. Clin. Invest.* **114,** 172–181
19. Ng, C. M., Cheng, A., Myers, L. A., Martinez-Murillo, F., Jie, C., Bedja, D., Gabrielson, K. L., Hausladen, J. M., Mecham, R. P., Judge, D. P., and Dietz, H. C. (2004) *J. Clin. Invest.* **114,** 1586–1592
20. Borges, M., Linnoila, R. I., van de Velde, H. J., Chen, H., Nelkin, B. D., Mabry, M., Baylin, S. B., and Ball, D. W. (1997) *Nature* **386,** 852–855
21. Sunday, M. E., and Cutz, E. (2000) in *Endocrinology of the Lung: Development and Surfactant Synthesis* (Mendelson, C. R., ed) pp. 299–336, Humana Press, Totowa, NJ
22. Cutz, E. (1982) *Exp. Lung Res.* **3,** 185–208
23. Hoyt, R. F., Jr., McNelly, N. A., McDowell, E. M., and Sorokin, S. P. (1991) *Am. J. Physiol.* **260,** L234–L240
24. Dakhama, A., Larsen, G. L., and Gelfand, E. W. (2004) *Curr. Opin. Pharmacol.* **4,** 215–220
25. Perl, A. K., Wert, S. E., Nagy, A., Lobe, C. G., and Whitsett, J. A. (2002) *Proc. Natl. Acad. Sci. U. S. A.* **99,** 10482–10487
26. Wuenschell, C. W., Sunday, M. E., Singh, G., Minoo, P., Slavkin, H. C., and Warburton, D. (1996) *J. Histochem. Cytochem.* **44,** 113–123
27. Ito, T., Udaka, N., Yazawa, T., Okudela, K., Hayashi, H., Sudo, T., Guillemot, F., Kageyama, R., and Kitamura, H. (2000) *Development* **127,** 3913–3921
28. Kazanjian, A., Wallis, D., Au, N., Nigam, R., Venken, K. J., Cagle, P. T., Dickey, B. F., Bellen, H. J., Gilks, C. B., and Grimes, H. L. (2004) *Cancer Res.* **64,** 6874–6882
29. Linnoila, R. I., Jensen-Taubman, S., Kazanjian, A., and Grimes, H. L. (2007) *Lab. Invest.* **87,** 336–344
30. Linnoila, R. I. (2006) *Lab. Invest.* **86,** 425–444
31. Hiroshima, K., Iyoda, A., Shida, T., Shibuya, K., Iizasa, T., Kishi, H., Tanizawa, T., Fujisawa, T., and Nakatani, Y. (2006) *Mod. Pathol.* **19,** 1358–1368
32. Hoyt, R. F., Jr., Sorokin, S. P., McDowell, E. M., and McNelly, N. A. (1993) *Anat. Rec.* **236,** 15–22; Discussion 22–14
33. White, S. R., Hershenson, M. B., Sigrist, K. S., Zimmermann, A., and Solway, J. (1993) *Am. J. Respir. Cell Mol. Biol.* **8,** 592–596
34. Sunday, M. E., Hua, J., Dai, H. B., Nusrat, A., and Torday, J. S. (1990) *Am. J. Respir. Cell Mol. Biol.* **3,** 199–205
35. Sunday, M. E., Yoder, B. A., Cuttitta, F., Haley, K. J., and Emanuel, R. L. (1998) *J. Clin. Invest.* **102,** 584–594
36. Pan, J., Luk, C., Kent, G., Cutz, E., and Yeger, H. (2006) *Am. J. Respir. Cell Mol. Biol.* **35,** 320–326
37. Van Lommel, A. (2001) *Paediatr. Respir. Rev.* **2,** 171–176
38. Lawlor, D. A., Ebrahim, S., and Smith, G. D. (2004) *Diabetologia* **47,** 195–203
39. Walter, R. E., Beiser, A., Givelber, R. J., O'Connor, G. T., and Gottlieb, D. J. (2003) *Am. J. Respir. Crit. Care Med.* **167,** 911–916
40. Itkin-Ansari, P., Marcora, E., Geron, I., Tyrberg, B., Demeterco, C., Hao, E., Padilla, C., Ratineau, C., Leiter, A., Lee, J. E., and Levine, F. (2005) *Dev. Dyn.* **233,** 946–953
41. Gasa, R., Mrejen, C., Leachman, N., Otten, M., Barnes, M., Wang, J., Chakrabarti, S., Mirmira, R., and German, M. (2004) *Proc. Natl. Acad. Sci. U. S. A.* **101,** 13245–13250
42. McDowell, E. M., Hoyt, R. F., Jr., and Sorokin, S. P. (1994) *Cell Tissue Res.* **275,** 157–167
43. Schonhoff, S. E., Giel-Moloney, M., and Leiter, A. B. (2004) *Endocrinology* **145,** 2639–2644
44. Habashi, J. P., Judge, D. P., Holm, T. M., Cohn, R. D., Loeys, B. L., Cooper, T. K., Myers, L., Klein, E. C., Liu, G., Calvi, C., Podowski, M., Neptune, E. R., Halushka, M. K., Bedja, D., Gabrielson, K., Rifkin, D. B., Carta, L., Ramirez, F., Huso, D. L., and Dietz, H. C. (2006) *Science* **312,** 117–121